



**HAL**  
open science

## Sintering behavior and microstructural evolution of NbC-Ni cemented carbides with Mo<sub>2</sub>C additions

Mathilde Labonne, Jean-Michel Missiaen, Sabine Lay, Nerea García, Olivier Lavigne, Luis Fernando García, Elena Tarrés

► **To cite this version:**

Mathilde Labonne, Jean-Michel Missiaen, Sabine Lay, Nerea García, Olivier Lavigne, et al.. Sintering behavior and microstructural evolution of NbC-Ni cemented carbides with Mo<sub>2</sub>C additions. International Journal of Refractory Metals and Hard Materials, 2020, 92, pp.105295. 10.1016/j.ijrmhm.2020.105295 . hal-02888643

**HAL Id: hal-02888643**

**<https://hal.science/hal-02888643>**

Submitted on 3 Jul 2020

**HAL** is a multi-disciplinary open access archive for the deposit and dissemination of scientific research documents, whether they are published or not. The documents may come from teaching and research institutions in France or abroad, or from public or private research centers.

L'archive ouverte pluridisciplinaire **HAL**, est destinée au dépôt et à la diffusion de documents scientifiques de niveau recherche, publiés ou non, émanant des établissements d'enseignement et de recherche français ou étrangers, des laboratoires publics ou privés.

# Sintering behavior and Microstructural Evolution of NbC-Ni Cemented Carbides with Mo<sub>2</sub>C Additions

Mathilde Labonne<sup>1</sup>, Jean-Michel Missiaen<sup>1</sup>, Sabine Lay<sup>1</sup>, Nerea García<sup>2</sup>, Olivier Lavigne<sup>2</sup>, Luis Fernando García<sup>2</sup>, Elena Tarrés<sup>2</sup>

<sup>1</sup> Univ. Grenoble Alpes, SIMAP, Grenoble INP, Saint-Martin d'Hères, 38400, FRANCE.

<sup>2</sup> Hyperion Materials & Technologies SPAIN, Pol. Ind. Roca, C/ Veneda 12-24, Martorelles 08107 SPAIN

---

## Abstract

The effect of Mo<sub>2</sub>C additions to a NbC-12vol%Ni-0.5vol%WC material on sintering at 1450°C and on the resulting microstructure was investigated by replacing different amounts of NbC with Mo<sub>2</sub>C (0%, 3%, 6% or 9% in volume) and by performing interrupted tests at key temperatures (1080°C, 1180°C and 1320°C). Chemical reactions and phase transformations were followed by Thermogravimetric Analysis (TGA) and sintering behavior by dilatometry. The microstructure was studied by Scanning and Transmission Electron Microscopy (SEM and TEM), Energy Dispersive Spectrometry (EDS) and X-ray diffraction (XRD). It is observed that Mo<sub>2</sub>C and WC particles, present at the onset of solid state sintering, delay the shrinkage of the material. An increase of hardness with Mo<sub>2</sub>C addition is measured, mainly due to grain refinement.

## Keywords

Niobium, Carbide, Sintering, Binder, Nickel

## 1. Introduction

WC-Co cemented carbides are the most widely used material for wear application due to their excellent hardness, toughness and strength [1]. However, several factors, such as the price increase of both major elements, cobalt and tungsten [2], and new toxicology regulations regarding cobalt [3], lead industrials to consider alternative materials to WC-Co.

A possible alternative is to combine niobium carbide and nickel. Like tungsten, niobium is from the groups IVB to VIB in the periodic table that are known to give very hard carbides, superior to most minerals. In the past, little attention has been drawn to niobium carbides since the 1970s studies by R. Warren [4][5][6], probably because of the availability and costs at the time, and because of the lower mechanical properties obtained for NbC-Co materials compared to WC-Co materials [7]. However, nowadays stocks and resources of niobium are significant, notably in Brazil [8], and it is therefore more and more attractive for companies to consider niobium containing materials. In order to produce NbC based hardmetals, it is necessary to select a binder. Cobalt is not an ideal choice because of its significant health risks. A considered alternative could be nickel as it is not classified as a hazardous material, and as it has a good wetting ability toward niobium carbides [5].

Previous studies have shown that a combination of NbC and Ni alone could not lead to very good mechanical properties [9][10]. This is mostly explained by an important grain size due to an uncontrolled grain growth during the sintering process. In order to limit this phenomenon, secondary carbides can be added. Several carbides were previously considered with NbC based materials such as WC [11][12], Mo<sub>2</sub>C [9] [10] [12], VC [9][10][12][13], or a combination of these carbides plus TiC [9][10][14]. Carbide additions efficiently inhibit grain growth, thus obtaining a finer microstructure and a better hardness. Good hardness-toughness combinations were also obtained for additions of a mix of secondary carbide such as VC-Mo<sub>2</sub>C [10] or Mo<sub>2</sub>C-VC-WC [12]. A core-rime structure was observed with combined additions of TiC and

Mo<sub>2</sub>C, or TiC and VC [9]. Those studies all focused on the effect of secondary carbide additions on the final microstructure and mechanical properties, without investigating thoroughly sintering in itself.

In a previous study, Huang et al [15] have showed that WC has a significant effect on grain growth. In this work, the WC content has been fixed at 0.5vol% and the effect of additions of Mo<sub>2</sub>C as a secondary carbide on the sintering, microstructure and mechanical properties in a NbC-Ni material is studied. NbC-Ni alloys with various Mo<sub>2</sub>C additions are prepared by conventional sintering under vacuum. Microstructural evolution is discussed from SEM, TEM and EBSD analyses.

## 2. Experimental

### 2.1. Materials preparation

The reference composition for this study is NbC-12vol%Ni-0.5vol%WC. Mixtures where a volume fraction of niobium carbide (3%, 6% or 9%) was replaced by the corresponding volume fraction of molybdenum carbide (Mo<sub>2</sub>C) were also prepared. These compositions are presented in Table 1.

**Table 1 - Nominal compositions to study the effect of secondary carbide addition (vol%).**

Name	NbC	Ni	Mo <sub>2</sub> C	WC	Total
Reference	87.5	12.0	0	0.5	100.0
3%Mo <sub>2</sub> C	84.9	12.0	2.6	0.5	100.0
6%Mo <sub>2</sub> C	82.2	12.0	5.3	0.5	100.0
9%Mo <sub>2</sub> C	79.6	12.0	7.9	0.5	100.0

To prepare these compositions, the following raw powders with their FSSS particle size were used: NbC (1.45 μm), Ni (2.55 μm), WC (3.8 μm) and Mo<sub>2</sub>C (1.8 μm). Their morphology is presented in Figure 1. Raw materials were obtained from Hyperion Materials & Technologies.

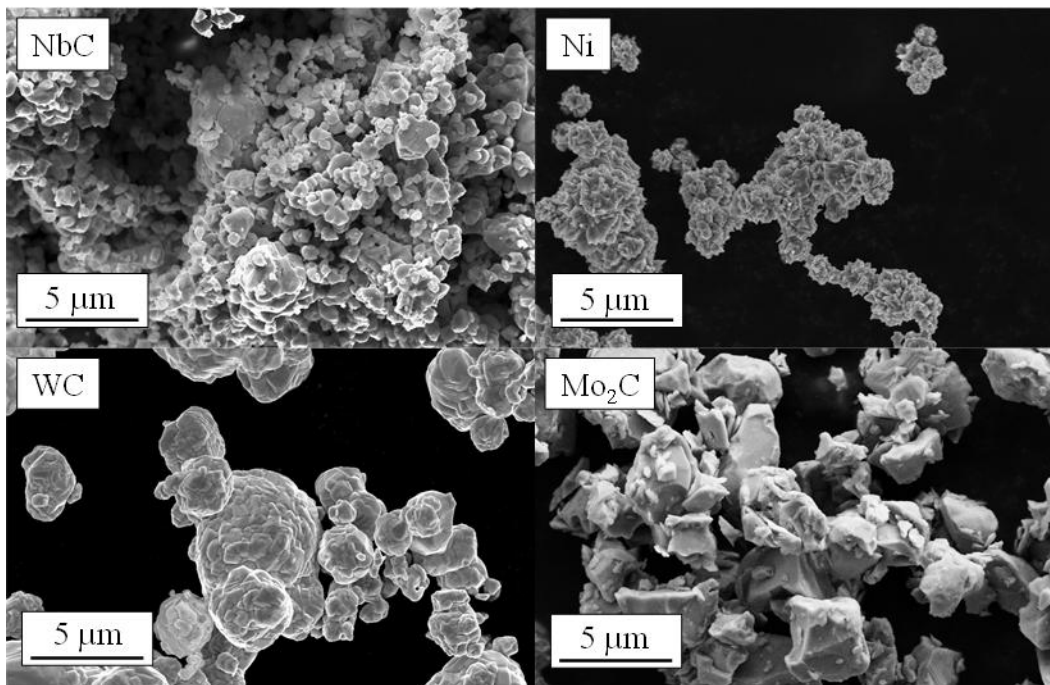


**Figure 1 - SEM image (secondary electrons) of the raw powders used to prepare the mixes.**

For each composition, raw materials and organic pressing agents were ball milled and dried at lab scale. An example of a granulated powder is presented in Figure 2. Cylindrical powder compacts (5.9 mm in height, 8 mm in diameter)

were obtained by uniaxial compaction to a relative 55% density by adjusting the uniaxial pressure, then debinded below 500°C for 1h with hydrogenated helium to eliminate pressing agents and possible hydroxides. Finally, a standard sintering is applied by heating at 6°C/min to 1450°C, then immediately cooling when reaching 1450°C at 20°C/min to 20°C in vacuum ( $5.10^{-6}$  bar).

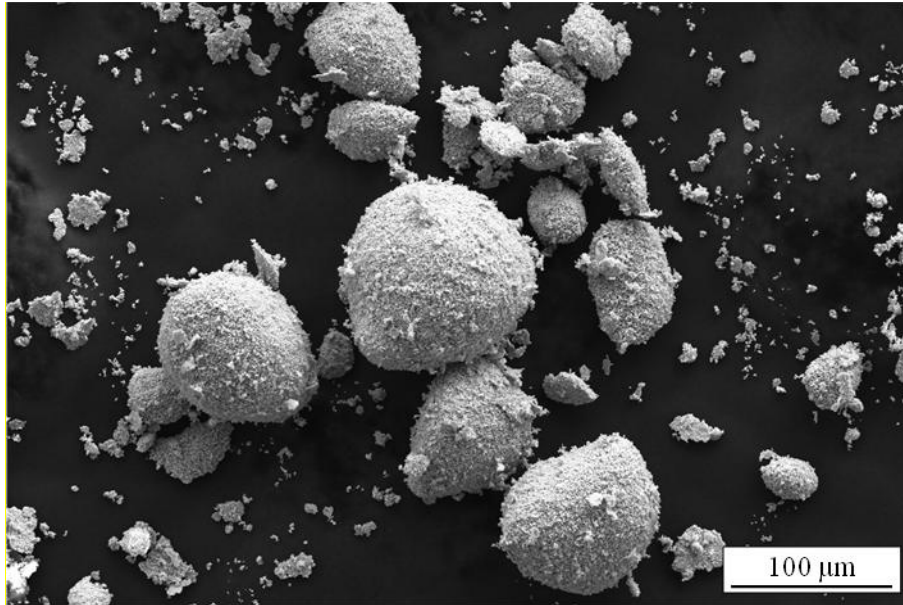


Figure 2 - SEM image of (NbC-3%Mo<sub>2</sub>C)-12vol%Ni-0.5vol%WC granulated powder mix with pressing organic agents.

## 2.2. Characterization

Chemical reactions and phase transformations were followed by Thermogravimetric Analysis (TGA) (Setaram Setsys 16/18) and sintering by dilatometry (Setaram Setsys Evolution 16/18) using the standard thermal cycle in vacuum described in section 2.1. The microstructure of the sintered samples was studied by XRD (PANalytical X'Pert Pro MPD), SEM (FEG-Zeiss Ultra 55), TEM (Jeol 3010 - 300 kV) and STEM (Jeol FEG 2100F - 200kV) equipped with EDS detectors. To study the grain boundary segregation, STEM/EDS maps were acquired using a beam size of 1 nm, a magnification of 500 000 and a map size of 512x512 or 256x256 pixels, resulting in a pixel size of 0.5 or 1 nm. The segregation width in the boundaries was estimated using a semi-quantitative method [16]. The hardness was measured by Vickers macrohardness with an indentation load of 30 kg. The toughness  $K_{Ic}$  was calculated from the crack lengths at the corners of each indentation using the relation of ISO 28079:2009 [17].

## 3. Results

### 3.1. Dilatometry and TGA measurements

The shrinkage  $\Delta h/h_0$  referred to the initial height  $h_0$  of the powder compact has been studied by dilatometry with various amounts of Mo<sub>2</sub>C. All samples are fully dense after sintering. The global shrinkage at the end of the sintering varies between 19% to 21% as presented in Figure 3(a). The two major sintering steps can be identified on the shrinkage rate curves presented in Figure 3 (b): the first broad peak (I) corresponds to solid state sintering and the second narrow peak (II) at about 1300°C to the liquid phase sintering. A third peak is visible at cooling around 1320°C, which corresponds to the solidification of the binder phase. When adding Mo<sub>2</sub>C, solid state sintering is significantly delayed to higher temperatures. It seems that the liquid phase sintering peak is slightly delayed toward higher temperature when adding Mo<sub>2</sub>C, but this may be due to the more important overlap between the solid state sintering and liquid phase sintering peaks when adding Mo<sub>2</sub>C. Therefore, we cannot conclude on a possible effect of Mo<sub>2</sub>C on the liquid phase sintering temperature.

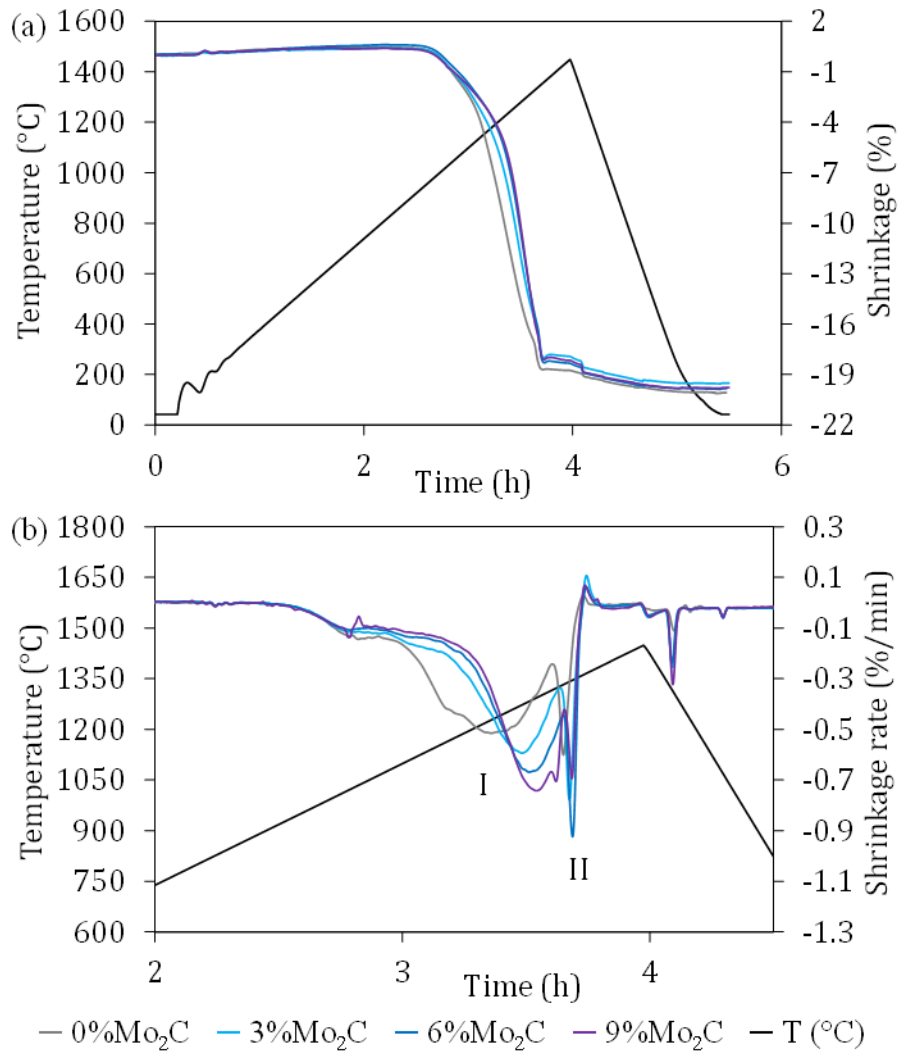


**Figure 3 - Dilatometry curves of powder compacts with different Mo<sub>2</sub>C content. (a) Shrinkage (%), (b) Shrinkage rate (%/min) showing the different sintering steps: I. Solid state sintering, II. Liquid phase sintering.**

The results of the mass loss measurements obtained by TGA after the debinding step are presented in Figure 4. The mass loss varies between 1.3% and 1.4%. The 3%Mo<sub>2</sub>C composition seems to have a more important mass loss than the other compositions. However, the mass loss for this composition starts before 400°C, suggesting that the debinding step was not complete for this sample. Otherwise, the mass loss during sintering seems to be about the same for all compositions (1.3%), indicating that the Mo<sub>2</sub>C addition has no significant effect on mass loss. Two peaks are observed on the mass loss rate curve: a first peak around 850°C (A) attributed to Nb/Mo/W oxide reduction and a second peak at 1340°C (B) to nickel evaporation. **Nickel oxides are reduced at low temperature during debinding (see Ellingham diagram [18]).** The quantity of nickel evaporated is about 0.4wt% and is similar for all compositions, therefore its potential effect on the microstructure will not be taken into account.

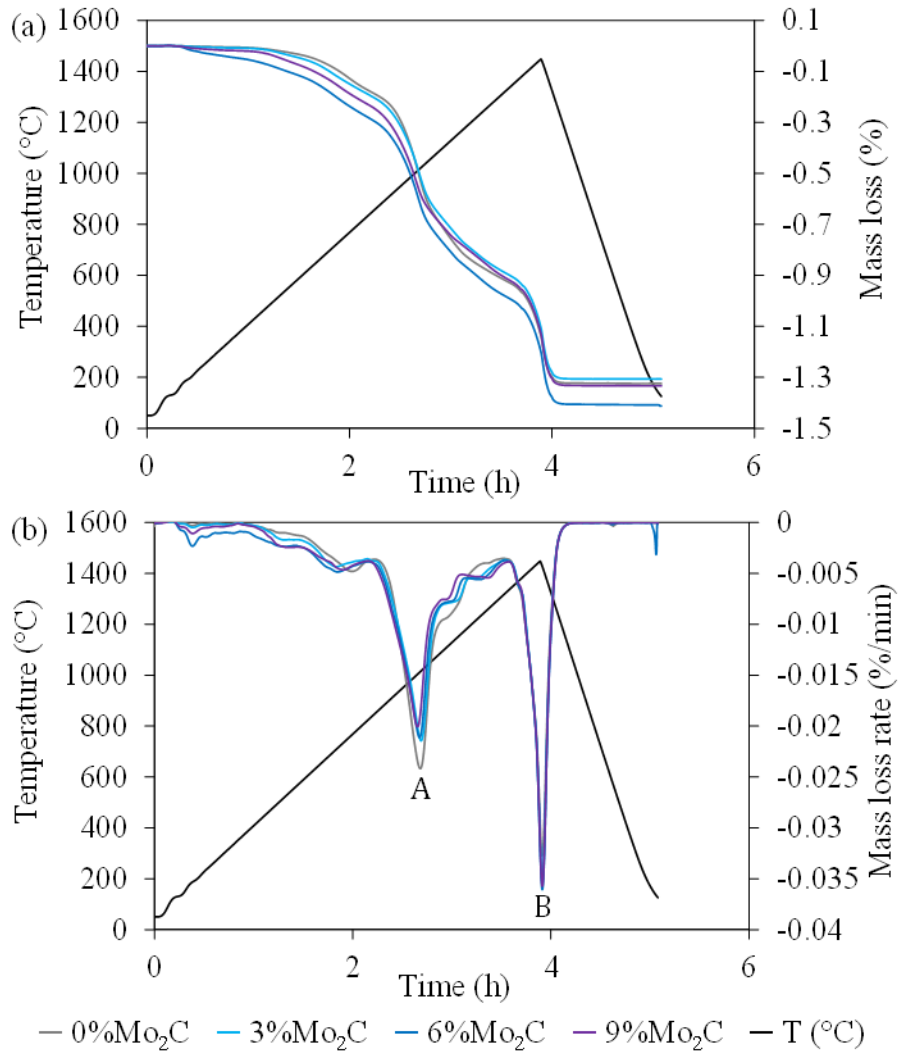


**Figure 4 – Thermogravimetric plots of powder compacts with different Mo<sub>2</sub>C contents during the standard sintering cycle, (a) Mass loss (%), (b) Mass loss rate (%/min).**

### 3.2. Microstructural study of sintered alloys

For the reference composition NbC-12vol%Ni-0.5vol%WC, two phases are visible as presented in Figure 5: NbC carbides and a nickel-rich binder. The EDS mapping shows the repartition of niobium and nickel.

A more detailed STEM/EDS analysis of a 6%Mo<sub>2</sub>C sample (Figure 6) shows that niobium is found in small quantities in the binder, but no nickel is detected in the carbides. The average composition of each phase measured by STEM/EDS on a 9%Mo<sub>2</sub>C sample is presented in Table 2. Note that the small amount of Ni found in the carbide grains is probably due to binder re-deposition on the TEM specimen during the Ar ion milling step. No core-rim structure in the NbC grains is observed. A nickel segregation is observed by EDS at grain boundaries as presented in Figure 6(b), indicating the good wetting of the carbides by the nickel-rich binder. The segregation width was estimated to be close to 0.2 nm (1 monolayer).

Some defects are visible inside the carbide grains: either holes or binder inclusions (Figure 6(c)). The inclusions at the triple junctions and inside the grains are confirmed to be binder inclusions. It is also observed by TEM that these inclusions have a cube/cube orientation associated with a parametric misfit of 22% with the surrounding grain as presented in Figure 7.

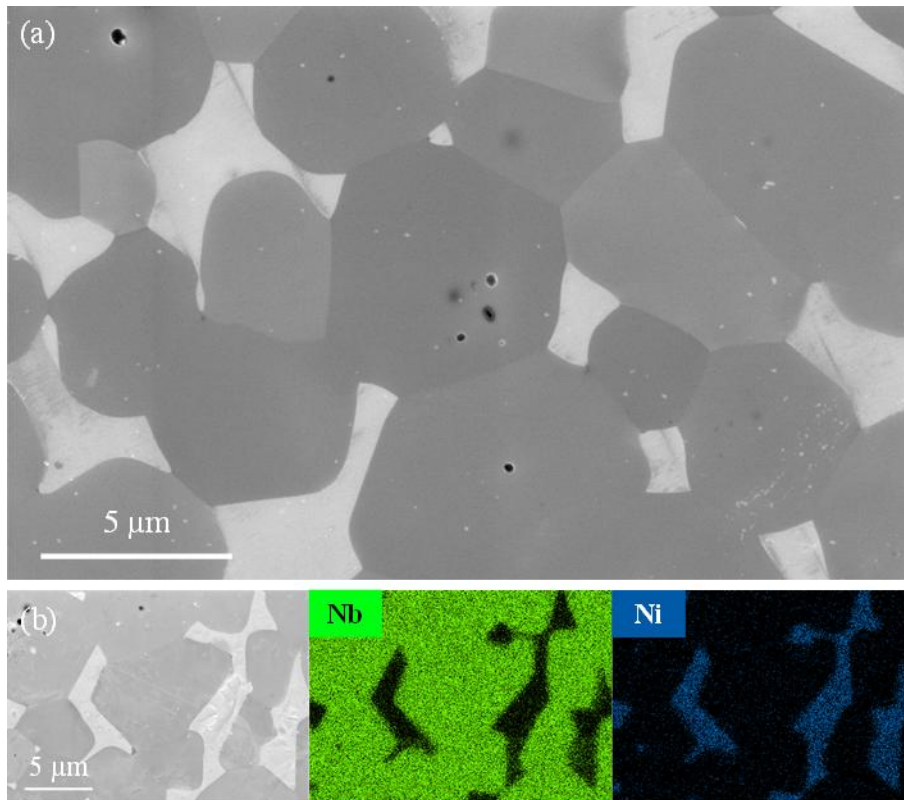


Figure 5 – 0%Mo<sub>2</sub>C compact sintered with the standard cycle, (a) SEM image (secondary electron), (b) SEM image & EDS mapping.

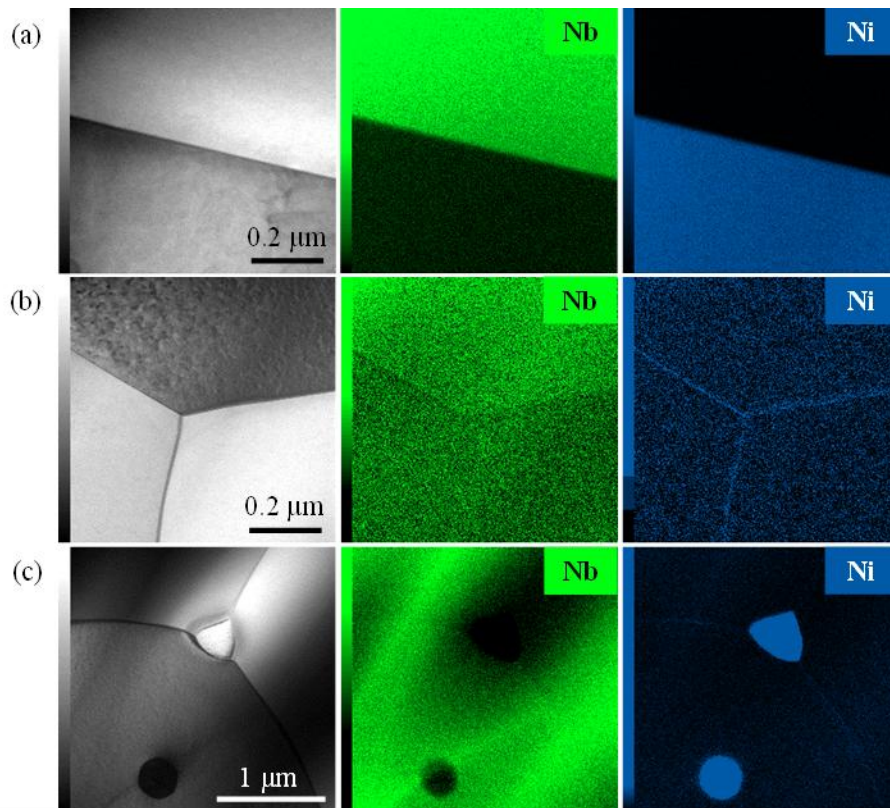
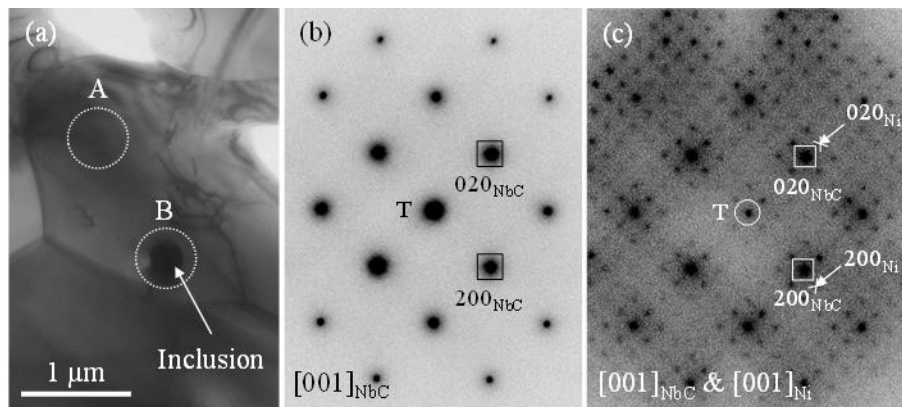


Figure 6 - TEM-EDS study of 6%Mo<sub>2</sub>C sample, (a) Interphase carbide-binder, (b) Triple grain boundary, (c) Intragranular defect & binder inclusion at triple grain boundary.

Table 2 - Average compositions measured by STEM/EDS in a 9%Mo<sub>2</sub>C sample (at%), carbon excluded.

Phase	Nb	Ni	Mo	W	Total
Carbide	94.3	0.4	5.0	0.3	100.0
Binder	5.7	86.7	6.8	0.8	100.0



**Figure 7 - TEM image and diffraction pattern of a Ni inclusion in NbC grain in the 6%Mo<sub>2</sub>C alloy, (a) TEM image of the area of analysis, (b) Electron diffraction pattern of cubic NbC in region A viewed along [001]<sub>NbC</sub>, (c) Diffraction pattern of NbC in region B with Ni inclusion depicting a cube-cube relation. The additional reflections are due to double diffraction.**

The microstructure of NbC-12vol%Ni-0.5vol%WC sintered compacts with different amounts of Mo<sub>2</sub>C additions is shown in Figure 8. First, the same two phases microstructure is visible for all compositions: a carbide phase and a nickel-rich binder.

The XRD study (Figure 9) confirms the nature of the phases. This study, combined with Table 2, indicates that mixed (Nb,Mo)C are formed by adding Mo<sub>2</sub>C. Furthermore, when Mo<sub>2</sub>C is added, the measured value of NbC lattice parameter drops while the nickel lattice parameter increases.

Finally, the objective of the secondary carbide addition is reached as the grain size is significantly reduced when adding Mo<sub>2</sub>C. A quantitative study of grain size distributions will be carried out in the future.

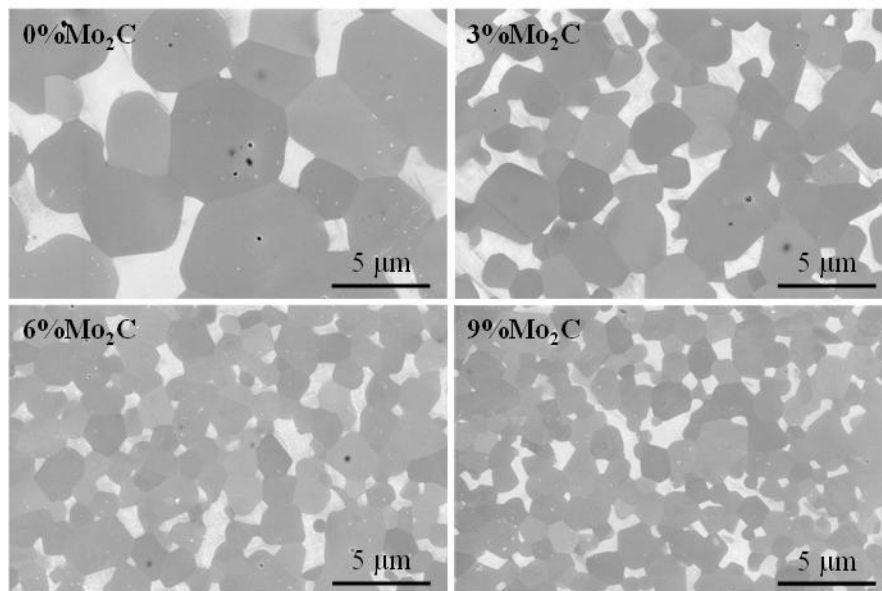


**Figure 8 - Secondary electron images of NbC-12vol%Ni-0.5vol%WC with different amounts of Mo<sub>2</sub>C**

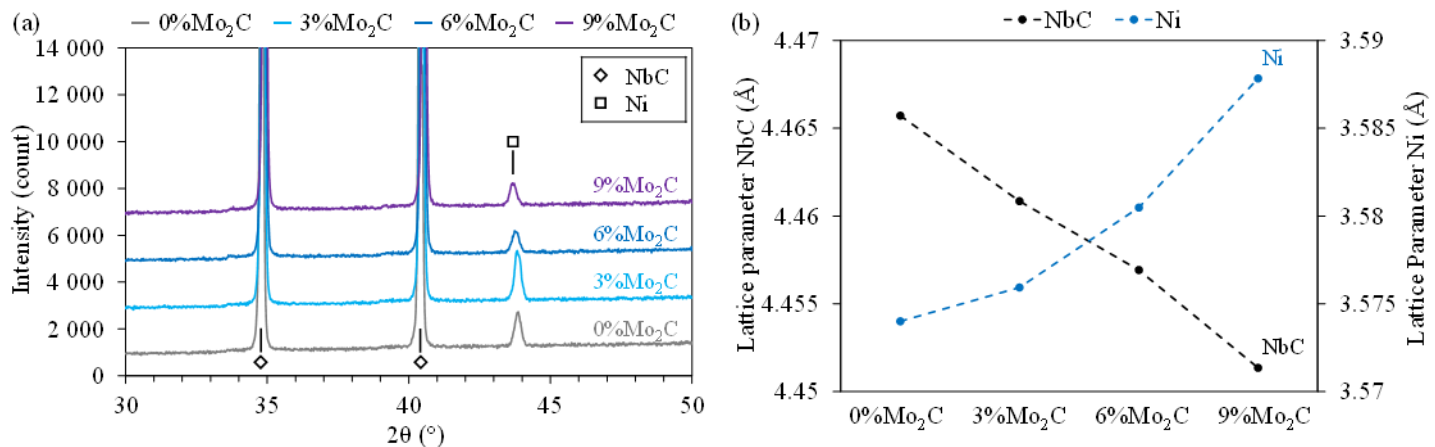


**Figure 9 – XRD study of compacts with different contents of Mo<sub>2</sub>C, (a) XRD pattern showing a NbC phase and a Ni phase, (b) Lattice parameters evolution of both phases depending on the Mo<sub>2</sub>C content.**

### 3.3. Microstructural study after interrupted tests

The sintering process was investigated by performing interrupted tests **without dwelling time** on 3%Mo<sub>2</sub>C compacts. Three temperatures have been selected (Figure 10): 1080°C and 1180°C, which corresponds to the beginning of solid state sintering without and with Mo<sub>2</sub>C additions respectively, and 1320°C, which corresponds to the intermediary step between solid state and liquid phase sintering with Mo<sub>2</sub>C.

The corresponding microstructures are presented in Figure 11. **At 1080°C and 1180°C, nickel agglomerates of a few μm are visible, and the carbide grain size remains small. A significant grain size increase is visible after solid state sintering at 1320°C, and also after the liquid phase sintering at 1450°C. The nickel binder has efficiently spread during solid state sintering, although a small porosity remains at 1320°C. This porosity is suppressed during liquid phase sintering.**

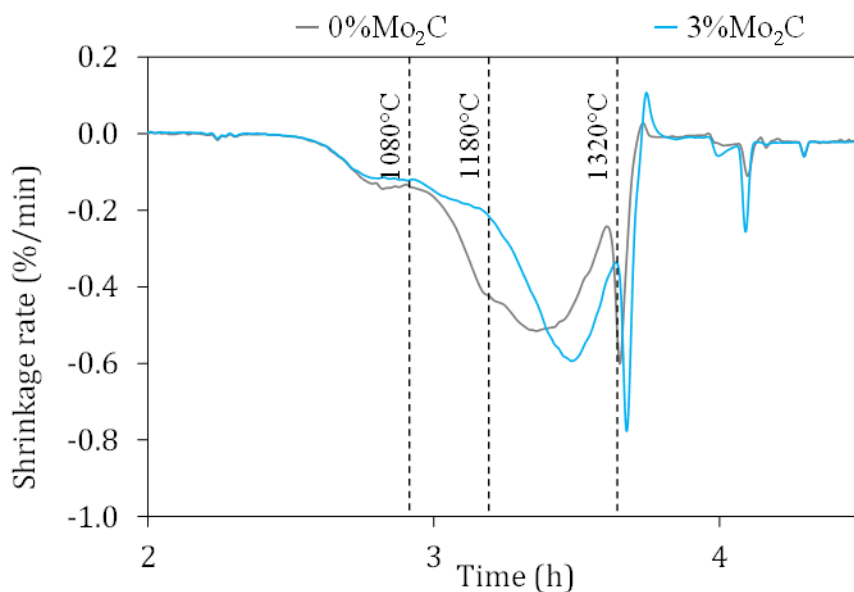


**Figure 10 - Shrinkage rate curve of 0%Mo<sub>2</sub>C & 3%Mo<sub>2</sub>C sintered with the reference cycle.**

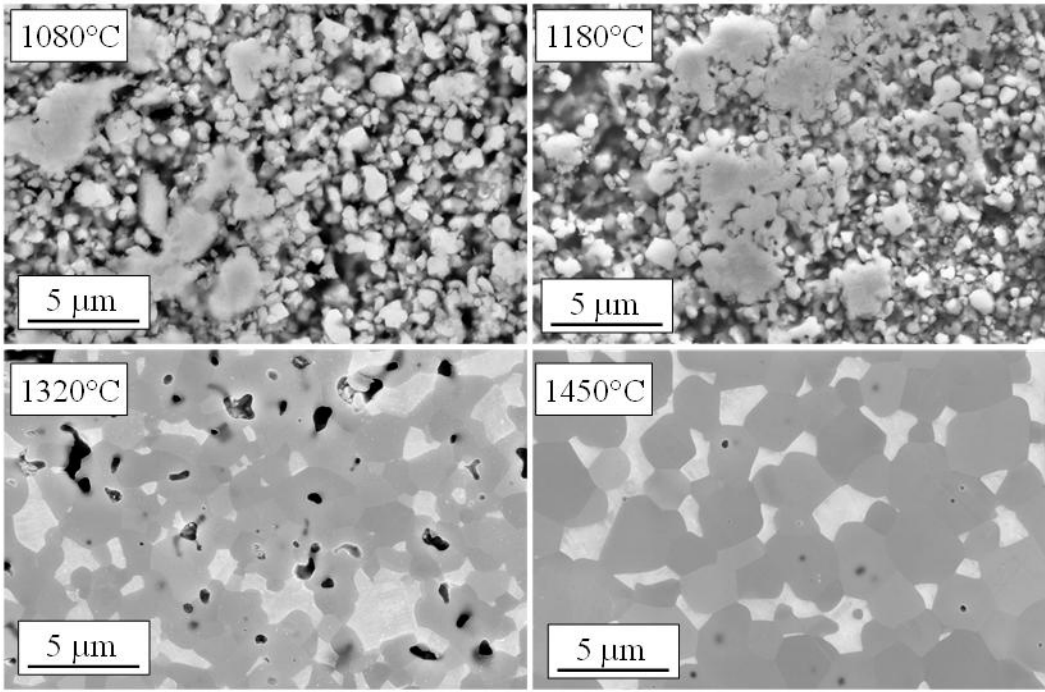


**Figure 11 – SEM images of 3%Mo<sub>2</sub>C samples sintered at different temperature (Secondary Electrons).**

XRD diffraction patterns at each temperature are presented in Figure 12 (a). Individual components of the initial powder mixture (NbC, Ni, Mo<sub>2</sub>C and WC) are still identified at 1080°C. The dissolution of WC and Mo<sub>2</sub>C between 1080°C and 1180°C is confirmed as the corresponding peaks seems no longer visible. A very small peak of Mo<sub>2</sub>C is however still identifiable at 1180°C, indicating that **very few** Mo<sub>2</sub>C carbides have not yet dissolved. At 1320°C and 1450°C, only a NbC-rich and a Ni-rich phases are detected.

The local chemical analysis mapping (EDS) are presented in **Figure 13 for the powder mix and** in Figure 14 for samples sintered at 1080°C, 1180°C, 1320°C and 1450°C. At 1180°C, right before the solid state sintering accelerates, Mo<sub>2</sub>C or WC are no longer detected by EDS, indicating that those carbides have mostly dissolved into the microstructure. W is detected in higher quantity into the binder at 1180°C, 1360°C and 1450°C. **Mo is dissolved both in the binder and carbide phase.**

The lattice parameters of the two phases are plotted as a function of temperature in Figure 12 (b). Between 1080°C and 1180°C, the lattice parameter of the Ni-rich phase increases considerably, then remains constant above 1180°C. The lattice parameter of the NbC-rich phase decreases gradually from 1080°C to 1450°C.

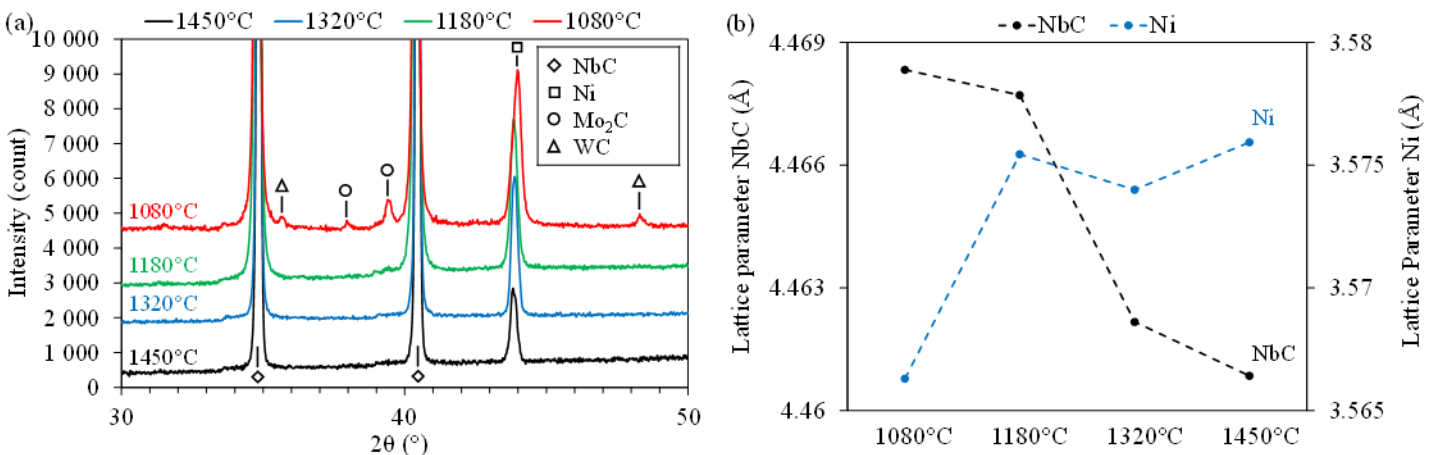


Figure 12 – (a) XRD pattern of 3%Mo<sub>2</sub>C samples sintered at different temperatures, (b) Lattice parameters of the NbC-rich and Ni-rich phases.

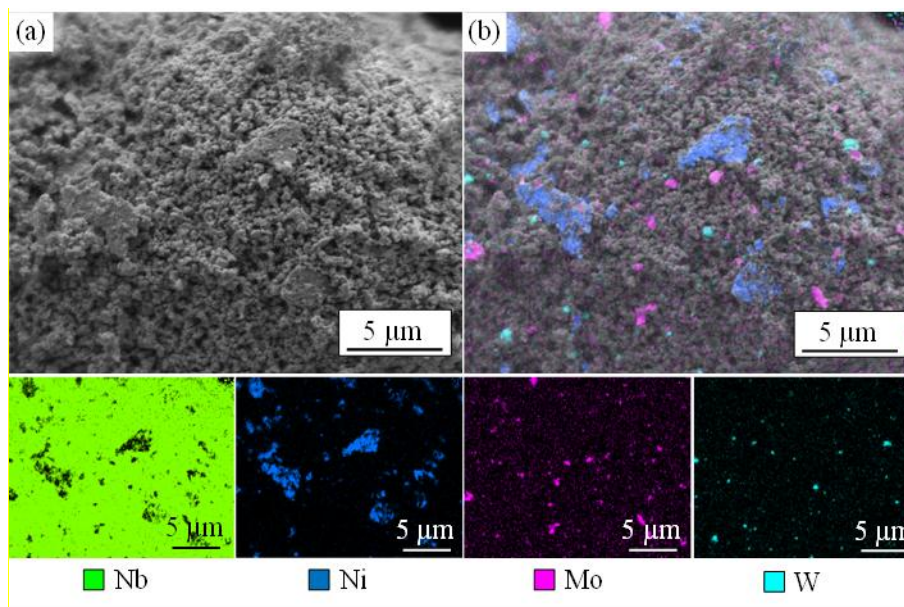


Figure 13 - SEM images and EDS mapping of (NbC-3%Mo<sub>2</sub>C)-12vol%Ni-0.5vol%WC powder mix with pressing organic agents, (a) Secondary electron SEM image, (b) EDS map of Ni, Mo and W superimposed on SEM image, (c) EDS map of Nb, Ni, Mo and W.

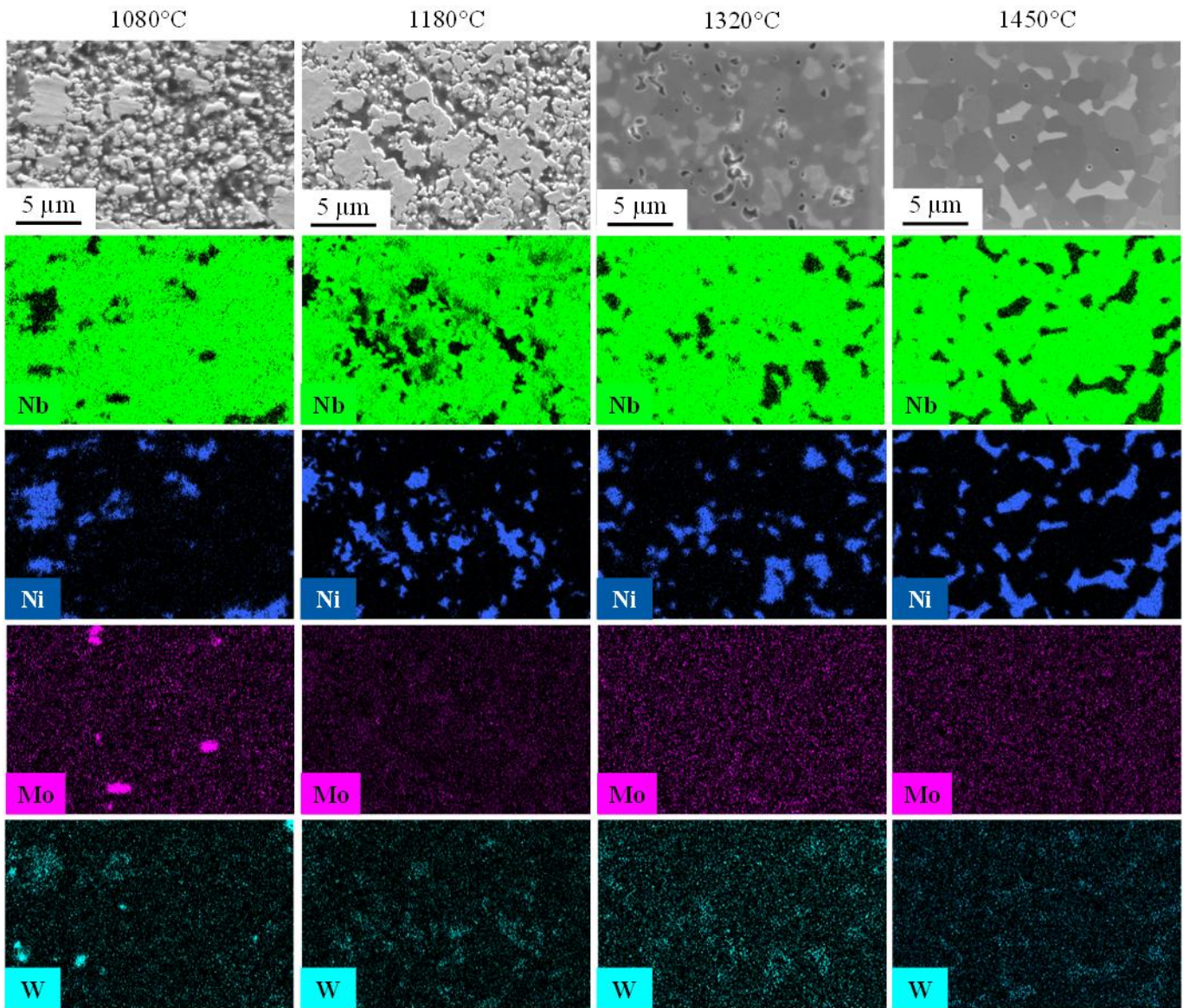


Figure 14 - EDS mapping of 3%Mo<sub>2</sub>C samples sintered at different temperature

### 3.4. Mechanical properties

The hardness and toughness of each composition were determined from HV<sub>30</sub> Vickers macro-indentations, as presented in Figure 15. The toughness could not be measured for the reference alloy as no cracks were formed because of the important grain size. Globally, the hardness increases and the toughness decreases when adding Mo<sub>2</sub>C.

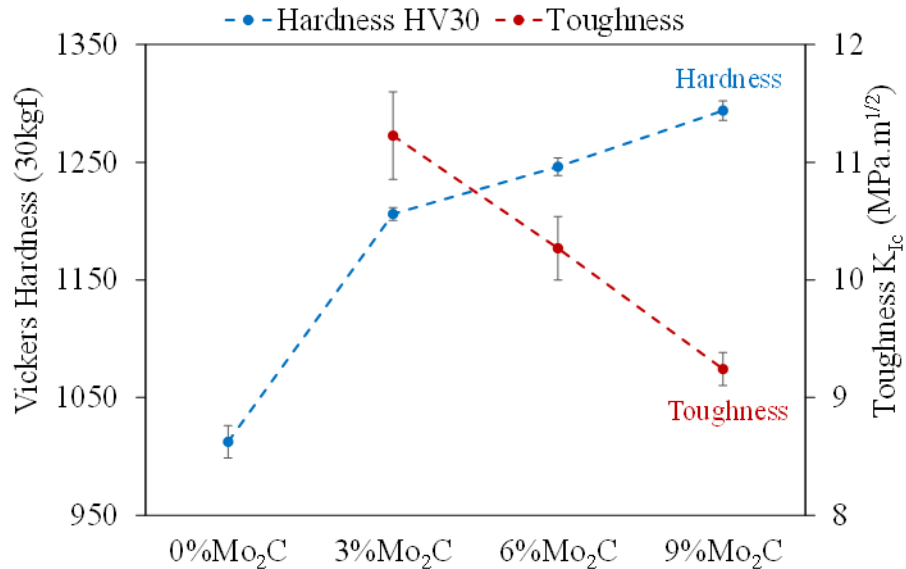


Figure 15 - Hardness and toughness of NbC-12vol%Ni-0.5vol%WC sintered materials with different amount of Mo<sub>2</sub>C.

#### 4. Discussion

This study aims to analyze the sintering behavior and resulting microstructure of a NbC-Ni material with and without secondary carbide addition of Mo<sub>2</sub>C.

First, the composition of the carbide and binder phases evolves during sintering. A small quantity of NbC is detected in the binder, as expected from the solubility value (7.0 wt% in nickel [19]). Mo<sub>2</sub>C dissolves in both NbC and nickel as expected from its good solubility in both phases (36 wt% in nickel [19] and 60 mol% in NbC [20]). With our experimental heating rate (6°C/min), Mo<sub>2</sub>C and WC dissolve into the carbide and binder phase during the first step of solid state sintering, between 1080°C and 1180°C. This temperature range would probably be higher if increasing the heating rate because of dissolution kinetics. As Mo<sub>2</sub>C and WC dissolve, the lattice parameter of the carbide and binder phases are affected. The atomic radius of molybdenum (190 pm) is smaller than the atomic radius of niobium (198 pm) but bigger than the atomic radius of nickel (149 pm) [21]. Therefore, the lattice parameter of the niobium-rich carbide phase decreases as Mo<sub>2</sub>C is added, while the lattice parameter of the nickel-rich phase increases. Tungsten, which has an atomic radius of 193 pm [21], dissolves preferentially into the binder and then also contributes to the increase of the binder lattice parameter. Between 1080°C and 1180°C, the lattice parameter of the Ni-rich phase significantly increases and remains virtually constant above 1180°C, whereas the lattice parameter of the NbC-rich phase mainly decreases above 1180°C. This is probably due to a slower diffusion kinetic of Mo and W in NbC than in Ni. The dissolution of Mo and W in NbC could have a positive effect on densification, as it should increase the affinity and then improve the wettability between the carbide and the binder phase [22].

Solid state spreading and sintering start as soon as the Nb/Mo/W oxides are reduced, as classically observed for cemented carbides [23]. However, a delay of the densification is observed for carbides with Mo<sub>2</sub>C addition. The onset of solid state sintering coincides with the end of the secondary carbide dissolution. These inclusions can be assumed to exert local tensile stresses on the neighboring NbC particles undergoing solid state sintering, which prevent shrinkage of the NbC skeleton [24]. This may also explain the apparent delay of liquid phase sintering as solid state sintering is not finished when the liquid forms. The densification is however still completed after liquid phase sintering.

The nickel segregation at grain boundaries attests the good affinity of Ni for NbC. The presence of binder inclusions or pores in the core of NbC grains in a system with a good carbide-binder wettability is unexpected [4] and could be explained by the initial heterogeneity of the powder mix. The local lack of nickel during solid state sintering could favor the coalescence of NbC clusters by grain boundary migration and entrap pores or solid binder inclusions, before the liquid phase is formed.

The hardness increases with Mo<sub>2</sub>C additions whereas the toughness decreases. These variations can be explained by the variations of the carbide grain size and by the higher solute content in the binder.

## 5. Conclusion

In this study, the sintering behavior as well as the microstructure of NbC-12vol%Ni-0.5vol%WC alloys with and without Mo<sub>2</sub>C additions were examined. Solid state sintering starts as soon as Nb/Mo/W oxides are reduced. The onset of solid state sintering is delayed in the presence of Mo<sub>2</sub>C/WC secondary carbide inclusions until they are dissolved, probably due to the tensile stresses they exert on the NbC skeleton. Mo<sub>2</sub>C and WC dissolve in the carbide and binder phases while NbC also dissolves in the binder. Mo<sub>2</sub>C additions have a clear inhibiting effect on NbC grain growth, already in the solid state. Work is still in progress to understand the mechanisms of grain growth inhibition.

## Acknowledgments

This research was performed in the framework of a research and development agreement between Hyperion Materials and Technologies – Grenoble INP – CNRS – Grenoble INP Entreprise. STEM/EDS was carried out at the CMTC characterization platform of Grenoble INP, supported by the Centre of Excellence of Multifunctional Architected Materials "CEMAM" n° ANR-10-LABX-44-01 funded by the "Investments for the Future" Program. G. Renou is acknowledged for his help at the 2100F JEOL microscope.

## References

- [1] J. Garcia, V. Collado Ciprés, A. Blomqvist, and B. Kaplan, Cemented carbide microstructures: a review, *Int. J. Refract. Metals Hard Mater.*, vol. 80, no. August 2018, pp. 40–68, 2019.
- [2] U.S. Geological, Metal Prices in the United States Through 2010, *Sci. Investig. Rep.*, no. 2012–5188, 2012.
- [3] National toxicology program, National Toxicology Program technical report on the toxicology studies of cobalt metal in F344/N rats and B6C3F1/N mice and toxicology and carcinogenesis studies of cobalt metal in F344/N rats and B6C3F1/N mice (inhalation studies), 2014.
- [4] R. Warren, Microstructural development during the liquid-phase sintering of two-phase alloys, with special reference to the NbC/Co system, *J. Mater. Sci.*, vol. 3, no. 5, pp. 471–485, 1968.
- [5] R. Warren, Carbide grain growth during the liquid-phase sintering of the alloys NbC-Fe, NbC-Ni and NbC-Co., *J. Less-Common Met.*, vol. 17, pp. 65–72, 1969.
- [6] R. Warren and M. B. Waldron, Microstructural development during liquid-phase sintering of cemented carbides. 1. Wettability and grain contact, *Powder Metall.*, vol. 15, no. 30, pp. 166–201, 1972.
- [7] R. Warren and H. Matzke, Indentation testing of a broad range of cemented carbides, in *Science of Hard Materials*, 1983, pp. 563–582.
- [8] A. R. Alves and A. dos R. Coutinho, The evolution of the niobium production in Brazil, *Mater. Res.*, vol. 18, no. 1, pp. 106–112, 2014.
- [9] S. G. Huang, J. Vleugels, H. Mohrbacher, and M. Woydt, NbC grain growth control and mechanical properties of Ni bonded NbC cermets prepared by vacuum liquid phase sintering, *Int. J. Refract. Metals Hard Mater.*, vol. 72, pp. 63–70, 2018.
- [10] S. G. Huang, J. Vleugels, H. Mohrbacher, and M. Woydt, Microstructure and tribological performance of NbC-Ni cermets modified by VC and Mo<sub>2</sub>C, *Int. J. Refract. Met. Hard Mater.*, vol. 66, no. March, pp. 188–197, 2017.
- [11] S. G. Huang, L. Li, O. Van der Biest, and J. Vleugels, Influence of WC addition on the microstructure and mechanical properties of NbC-Co cermets, *J. Alloys Compd.*, vol. 430, no. 1–2, pp. 158–164, 2007.
- [12] S. G. Huang, K. Vanmeensel, H. Mohrbacher, M. Woydt, and J. Vleugels, Microstructure and mechanical properties of NbC-matrix hardmetals with secondary carbide addition and different metal binders, *Int. J. Refract. Met. Hard Mater.*, vol. 48, pp. 418–426, 2015.
- [13] S. Huang, P. Baets, J. Sukumaran, H. Mohrbacher, M. Woydt, and J. Vleugels, Effect of Carbon Content on the Microstructure and Mechanical Properties of NbC-Ni Based Cermets, *Metals (Basel)*, vol. 8, no. 3, p. 178, 2018.
- [14] S. G. Huang, J. Vleugels, H. Mohrbacher, and M. Woydt, Microstructure and mechanical properties of NbC matrix cermets using Ni containing metal binder, *Met. Powder Rep.*, vol. 71, no. 5, pp. 349–355, 2016.
- [15] J. H. Huang, S. G. Huang, J. Vleugels, and B. Lauwers, Microstructure and mechanical properties of WC modified

- NbC-Ni cermets, in *Euro PM2019 - HM Microstructures*, 2019.
- [16] Z. Roulon, S. Lay, and J. M. Missiaen, Interface characteristics in cemented carbides with alternative binders, *Int. J. Refract. Met. Hard Mater.*, 2020.
- [17] ISO 28079:2009 Hardmetals — Palmqvist toughness test, 2009.
- [18] M. Hasegawa, *Ellingham Diagram*, vol. 1. Elsevier Ltd., 2013.
- [19] P. Ettmayer, H. Kolaska, W. Lengauer, and K. Dreyert, Ti(C,N) Cermets - Metallurgy and Properties, *Int. J. Refract. Met. Hard Mater.*, vol. 13, pp. 343–351, 1995.
- [20] G. S. Upadhyaya, Materials science of cemented carbides - an overview, *Mater. Des.* 22, pp. 483–489, 2001.
- [21] D. C. Ghosh and R. Biswas, Theoretical Calculation of Absolute Radii of Atoms and Ions . Part 1 . The Atomic Radii, pp. 87–113, 2002.
- [22] S. Lay and J. M. Missiaen, Microstructure and morphology of hard metals, *Compr. Hard Mater.*, vol. 1, no. 1.03, pp. 91–122, 2014.
- [23] J. Missiaen, Solid-state spreading and sintering of multiphase materials, *Mater. Sci. Eng. A*, vol. 475, pp. 2–11, 2008.
- [24] M. N. Rahaman, *Ceramic processing and sintering*, Marcel Dek. New York, 1995.